World Journal of Environmental Research
ISSN 2301-2641
Volume 14, Issue 2, (2024) 131-144
www.wjer.eu

Synthesis of Ag-ZnO/MOF nanocomposite for degradation of dye from aqueous solution under UV light

Hayder Mahmood Hameed [a1], Northern Technical University, 98XV+JR6, Mosul, Nineveh Governorate, 41002, Iraq., https://orcid.org/0000-0003-3340-2711
Israa Abbas Hasan [b], Northern Technical University, 98XV+JR6, Mosul, Nineveh Governorate, 41002, Iraq. israa3bbas91@gmail.com
Afrah Turki Awad [c], Northern Technical University, 98XV+JR6, Mosul, Nineveh Governorate, 41002, Iraq. afrah.turki@ntu.edu.iq, https://orcid.org/0000-0003-3967-0821

Suggested Citation:
Hameed, H.M., Hasan, I.A. & Awad, A.T. (2024). Synthesis of Ag-ZnO/MOF nanocomposite for degradation of dye from aqueous solution under UV light. *World Journal of Environmental Research*, *14*(2), 131-144. https://doi.org/10.18844/wjer.v14i2.9589

Received from April 8, 2024; revised from August 2, 2024; accepted from December 1, 2024.
Selection and peer review under the responsibility of Prof. Dr. Haluk Soran, Near East University, Cyprus

Abstract

Water pollution, a critical environmental challenge, threatens the availability of clean water essential for human survival. Industrial waste streams frequently discharge hazardous dyes such as Congo Red, Methyl Orange, and Methylene Blue, posing severe risks to aquatic ecosystems and human health. These dyes, widely used in industries like plastics, textiles, and cosmetics, contribute significantly to water contamination, necessitating effective treatment methods. This study addresses the research gap by synthesizing a silver-zinc oxide metal-organic framework (Ag-ZnO-MOF) nanocomposite for photocatalytic degradation of Methyl Orange dye using a chemical precipitation method. The nanocomposite's morphology, crystalline structure, and photocatalytic properties were characterized through SEM, FTIR, XRD, and DRS analyses, confirming its powdery nature and activity in the UV region with a bandgap of 3.3 eV. Key parameters influencing dye degradation, including solution pH, reaction time, pollutant concentration, and photocatalyst dosage, were systematically studied. The results revealed that optimal conditions (pH 2, 0.03 g photocatalyst, 30 ppm dye) achieved a remarkable 96% degradation efficiency. This research highlights the Ag-ZnO-MOF nanocomposite's potential for addressing industrial dye pollution, offering an effective and sustainable solution for water purification.

***Keywords*:** Dye removal; metal-organic framework; methyl orange; photocatalyst.

* Address for Correspondence: Hayder Mahmood Hameed, Northern Technical University, 98XV+JR6, Mosul, Nineveh Governorate, 41002, Iraq. *E-mail address*: haydermahmood@ntu.edu.iq

1. INTRODUCTION

One of the main environmental concerns in combatting pollution is the removal of hazardous substances from water resources (Suriadikusumah et al., 2021; Sharma & Sharma, 2021). However, this often gets polluted through the activities of man either directly or indirectly. Pollution of water resources with industrial effluents containing toxic pigments such as Congo red, methyl orange, and methylene blue, among others, is a serious problem for human health as well as the environment. Many of these dyes are poisonous and pose a serious hazard to aquatic animals and eventually, man who ends up consuming these.

There are several kinds of water pollutants, including Groundwater Pollution, Surface Water Pollution, Suspended Matter, Oil Spillages, Microbiological Pollution, Chemical Water Pollution, Thermal Pollution, and Oxygen-Depletion Pollution (Sheng & Webber, 2021). Thousands of different colors are used commercially in different industries such as plastics, cosmetics, paper and printing, textiles, and dyes to color various products. The process of producing colored products in industries uses a lot of water, which results in a huge amount of colored pollution (Srivastav et al., 2024).

The treatment for dye removal can be done through Biological, Physical, and chemical methods (Latif et al., 2024; Hashem et al., 2024). Photocatalysts are considered green or environmentally friendly (Gao et al., 2024). These materials can be activated by light, which leads to the breakdown of organic contaminants into small, non-poisonous molecules like H_2O and carbon dioxide (Kiteto et al., 2024). Photocatalytic appearances have their origins in photochemistry, heterogeneous catalysis, molecular spectroscopy, solid-state physics, materials science, and semiconductor surface science.

1.1. Literature review

1.1.1. Photocatalysis

Few semiconductors possess a bandgap in the range of 1.4 to 3.9 eV, corresponding to light wavelengths between 318 and 886 nm. However, not all semiconductors within this range are suitable for photocatalytic reactions. The most effective photocatalysts should be optimized for interactions between light and chemical processes while ensuring they contain no harmful constituents, particularly for applications in environmental studies. As illustrated in Figure 1, the mutual influence of physical fields plays a crucial role in enhancing photocatalytic efficiency, highlighting the intricate interplay of factors that govern the process.

Figure 1
The hierarchical structure of physics subfields

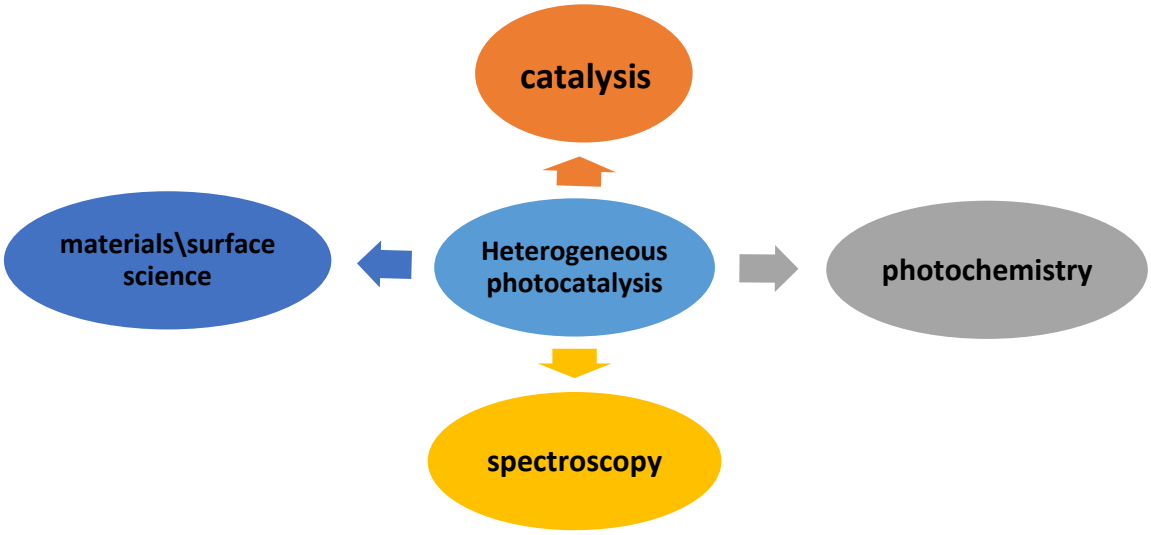

The title of Photocatalysis indicates that the reactions in which photons are absorbed by a solid remain unchanged during the entire reaction, causing a chemical change in the surrounding compounds. Among several methods, the photocatalytic properties of semiconductor oxides can be upgraded by increasing their

surface activity, reducing their band gaps, and using photoactive organic dyes to sensitize inorganic semiconductor surfaces. When the energy of the photon radiation is equal to or higher than slightly the band gap of the photocatalyst, electron-hole pairs are created with conduction band electrons as well as valence band holes.

Electron-hole pair generation was done with the required energy that was reached through light. The reaction with the environment takes place when electrons and holes are placed on the surface of the photocatalyst. Therefore, when the relocation time of electrons and holes to the photocatalyst surface is less than the re-combination time, the competence of the photocatalytic process will be higher.

Figure 2

Processes that happen after absorption of suitable radiation in a semiconductor

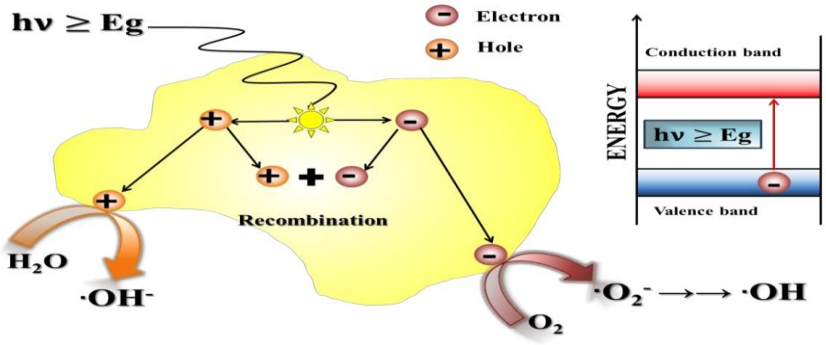

1.1.2. Efficiency of photocatalysts

Photoactive semiconductor materials are commonly utilized to purify water and air by degrading harmful organic substances such as dyes, carboxylic acids, aromatic compounds, pesticides, and many others. For instance, photocatalytic reactions are employed in generating hydrogen via water splitting, indicating a viable energy source, and in decomposing organic putrefaction on exposed elements such as glass window panes. Figure 3 is a comparison of the performance of natural photocatalysts and synthetic photocatalysts.

Figure 3

Natural (Top) and artificial photosynthesis

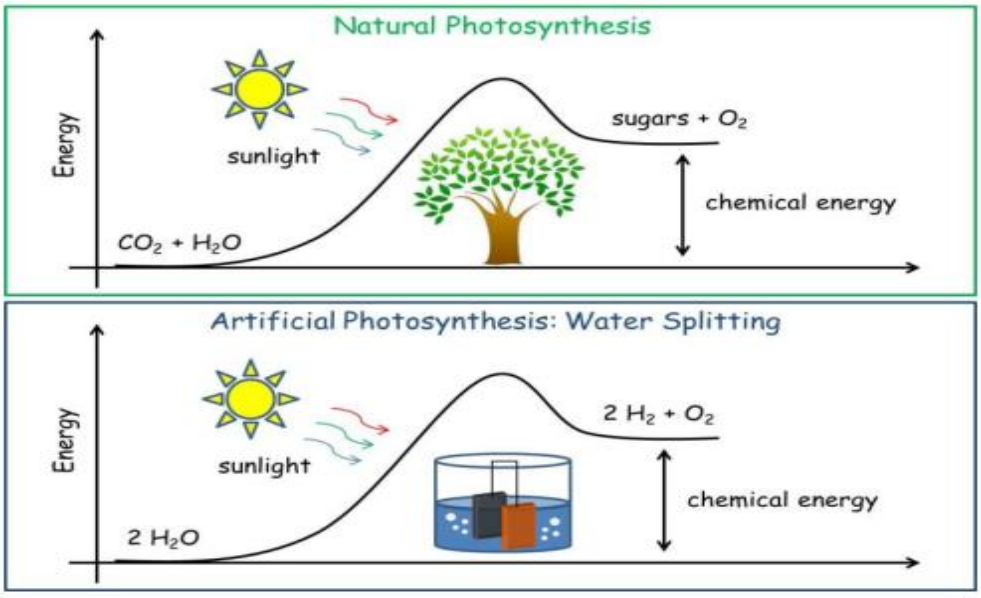

Additionally, semiconductor oxides have comfortable physical properties leading to their widespread use in photocatalytic processes. In addition to the activity of light photocatalysts used in environmental applications, some other essential criteria should be fulfilled, such as non-toxicity, chemical stability, and environmental compatibility. The lowest value for electrical conductivity of a solid-state is obtained only from electrons in half-filled orbitals filling them leads to the formation of the conduction band. In metals, the conduction and valence bands overlap, which allows the conduction band to be easily filled (see Figure 4).

Figure 4

Categorization of solid-state materials based on their electronic structure (theory)

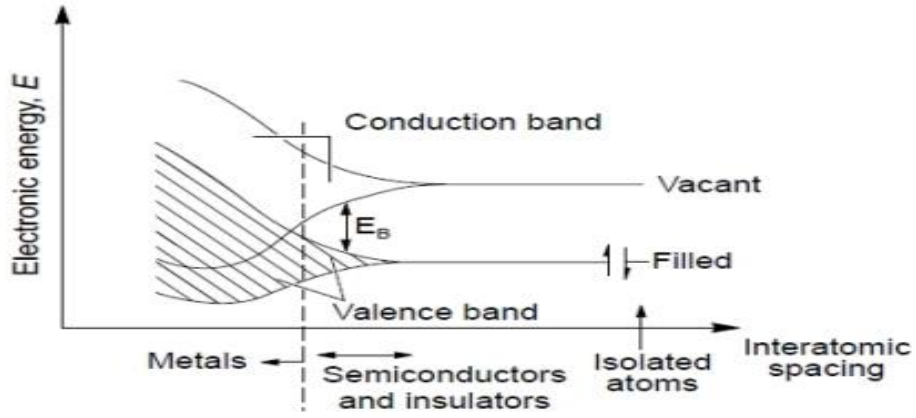

In insulators, the band gap is so large that electrons do not spontaneously move from the valence band to the conduction band. In semiconductors, however, the band gap is smaller, allowing for electrons to be excited into the conduction band. When electrons move from the valence band to the conductance band it creates a hole in the valence band. These holes are positively charged vacancies that are also able to move by capturing an electron into their vacancy. It also makes holes mobile so they can go anywhere. The conduction band has photochemically or thermally excited electrons (Figure 5).

Figure 5

Electron-hole pair production

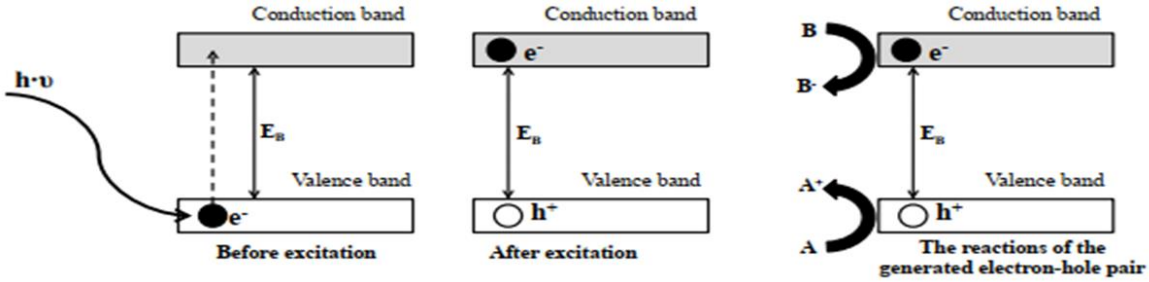

1.1.3. Metal-organic frameworks (MOF)

Metal-organic frameworks (MOFs) are a type of crystalline and porous materials that consist of inorganic building blocks, termed secondary building units (SBU), held together by multifunctional organic ligands (Figure 1-10)1. The high specific surface area is considered one of the vital features of MOFs that enhance their superior gas storage potential. For the assembly into coordination compounds, the composition of the monomers relies on the interactions between metal cations, e.g. Zn^{2+} ions (blue) and 1,4-benzene dicarboxylic acid (H_2bdc) (gray) → MOF-5 (Figure 1-10, top left). * Or one can use another ligand, e.g. 2-methylimidazole (pale green), with the same metal to get the ZIF-8 structure (Figure 6 top right). For example, similarly with Zr^{4+} (green) SBU using the same ligand (H_2bdc) presents a completely different structure called UiO-66. For

example, in the case of the structurally similar UiO-66/67 pair (bottom), the volume of the ligand (in this case, to add 4,4'-biphenyl dicarboxylic acid (yellow) to the linker VOC), which acts to increase the distance between the coordination nodes of the framework, can be controlled and used to control the pore size of the resulting MOF.

Figure 6

Variation of metal-organic framework (MOF)

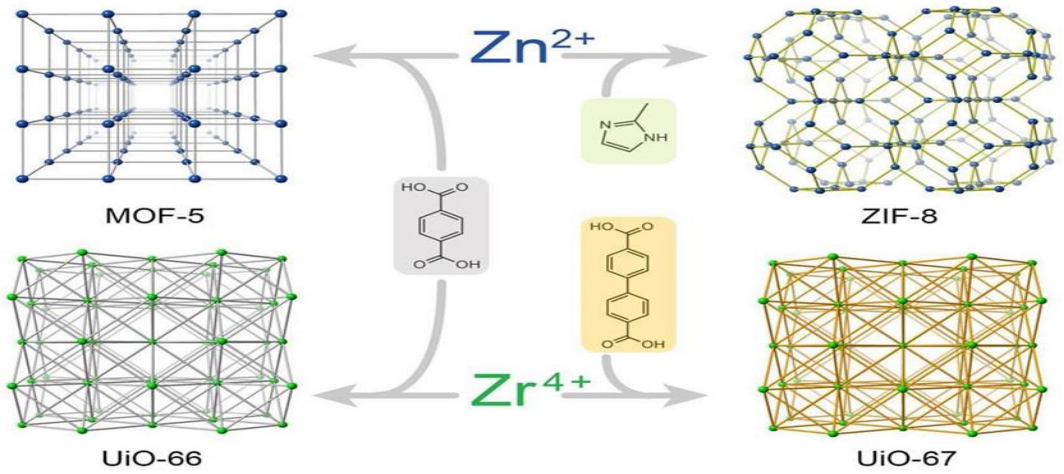

Images are modular which can be represented by a simple rod-and-sphere TIC model, wherein, the metal atoms act as the nodes or vertices of the metal-organic coordination frameworks while the organic ligands are represented by the rods connecting them (**Figure 7**).

Figure 7

Rod and sphere image of a MOF and its components

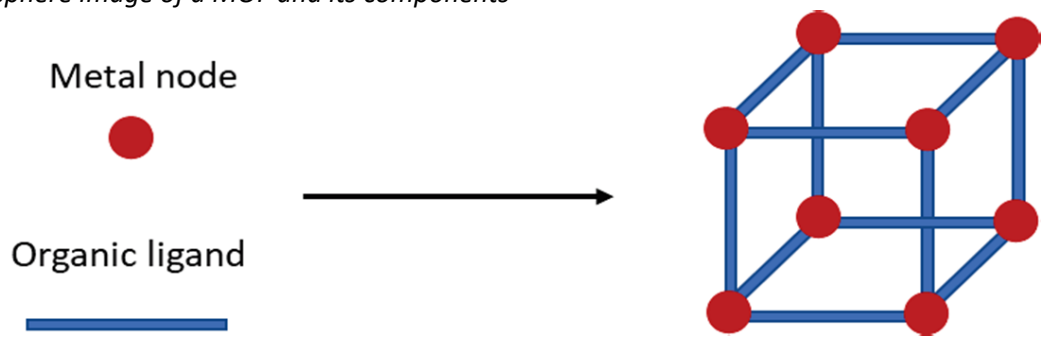

1.1.4. Separation technologies based on MOFs

Various formats based on new technologies, utilizing the unique properties of MOFs, show great promise for separations. MOFs can be synthesized with surface areas as high as 7,000 m^2/g and so are ideal for separation processes which are more difficult to achieve with other materials. The MOF network contains a combination of inorganic and organic components and the establishment of post-synthetic modification protocols enables tunability of physical and chemical properties. This flexibility makes MOFs the best candidate compared to other mineral films and mineral-doped membranes.

1.2. Purpose of study

The rapid increase in the number of harmful dyes in environmental pollution and their adverse effects on living beings, human health, plants, and soil, necessitates the need for efficient techniques that can eliminate these pollutants or convert them into less harmful forms. The reason for the investigation of the photocatalyst

method, in this research, is that it has economic and environmental advantages. Herein the study is aimed to synthesize Ag-ZnO/MOF nanocomposite through self-driven co-precipitation for the uptake of methyl orange dye and examination of its structure and surface morphology.

2. METHODS AND MATERIALS

Environmental pollutants have been extensively removed, reduced, or oxidized by nanoparticles (Singh et al., 2024). Among these materials, the Metal-Organic Frameworks (MOFs) represent highly chemically stable, low-cost materials that are also useful for photocatalysis to degrade pollutants. The following steps were performed in pursuit of this goal:

- Preparation of Ag-ZnO and MOF composites
- Application of the nanocomposite for dye removal
- Examination of relevant parameters affecting reduction like pH, time, initial concentration, and adsorbent dose.
- (k) Kinetics and stability study of photocatalyst

2.1. Materials

Table 1 shows the materials, manufacturer, and formula used for this study.

Table 1
Materials, manufacturer, formula

Material	Manufacturer	Formula
2-methylimidazole	Eldridge	**2-MeIM**
silver nitrate	Eldridge	**$AgNO_3$**
Zinc acetate	Sinopharm Chemical Reagent	**$Zn\ (COOH_3)_2{\cdot}2H_2O$**
methanol	Sinopharm Chemical Reagent	**MeOH**
sodium borohydride	Sinopharm Chemical Reagent	**NaBH4**

2.2. Specification of devices

Table 2 shows the specifications of the devices used for this study.

Table 2
Specification of devices

Device Type	Model	Manufacturing Country
Magnetic Stirrer	MS300HS	**Germany**
Digital scale	Helmer-FR200	**Germany**
Ultrasound	PSA100-SK1	**South Korean**
Shaker	Ika,260 Ks	**Germany**
Centrifuge	Z 206 A	**Germany**
Oven	Binder- FD 23	**American**
Spectrophotometer (UV-VIS)	ChromTech-UV1100	**Taiwan**

2.3. Synthesis methods

- **Preparation of MOF**

ZIF-8 was synthesized by chemical precipitation. The preparation method involved the dissolution of two different solutions (solution A and solution B) that contained 2.195 g of Zn $(CH_3COO)_2 \cdot 2H_2O$ and 6.489 g of 2-methylimidazole (2-MeIM), respectively, in methanol in 200 ml. Solution A was added to solution B under stirring for 1 h. The resulting mixture was collected and dried at 60 °C to obtain the ZIF-8 structures.

- **synthesis of Ag-ZnO Nanocomposite**

10 mg of $AgNO_3$ was dissolved in 10 ml deionized water and 80 mg of ZIF-8 was dissolved in 2 ml deionized water. A certain volume of $AgNO_3$ (0, 0.5, 1.0, and 2.0 ml) was titrated dropwise into ZIF-8 solution for preparing Ag-ZIF-8 composites with different silver content. The Ag^+ ions were reduced by a fresh $NaBH_4$ solution (1.5 mg/ml). ZnO nanoparticle was prepared as mentioned above by heating ZIF-8 powders at 600 degrees Celsius for 2 hours in the air. Ag-ZnO hollow nanocomposites were formed upon calcining Ag-ZIF-8 powders at 500°C for 2 h.

- **Preparation of methyl orange**

Methyl orange dye was used to prepare the effluent in the laboratory. To prepare 1 liter of solution with a concentration of 100 ppm, 100 mg of dye was dissolved in 1 liter of deionized water. Next, the required amount was taken from the stock solution for each test according to formula 1-3 and diluted.

3. RESULTS

3.1. Investigating the physicochemical properties of photocatalyst

3.1.1. FTIR

FTIR activities of the samples measured in the range of 400-4000 cm^{-1} were taken from zinc oxide doped with silver and then its nanocomposite form with MOF.

FTIR Analysis: The FTIR spectra of synthesized samples exhibited a broad absorption band at 3444 cm^{-1}which was assigned to O-H stretching of H_2O adsorbed on the surface of ZnO. Two extra peaks at 2974 cm^{-1} were attributed to C-H stretching in acetate species. The band at 429 cm^{-1} belonged to the Zn−O bond, and bands at 1384 and 1576 cm^{-1} were attributed to carboxylate groups of MOFS (figure 8).

Figure 8

FTIR analysis results for (a) Ag/ZnO and (b) MOF-Ag/ZnO

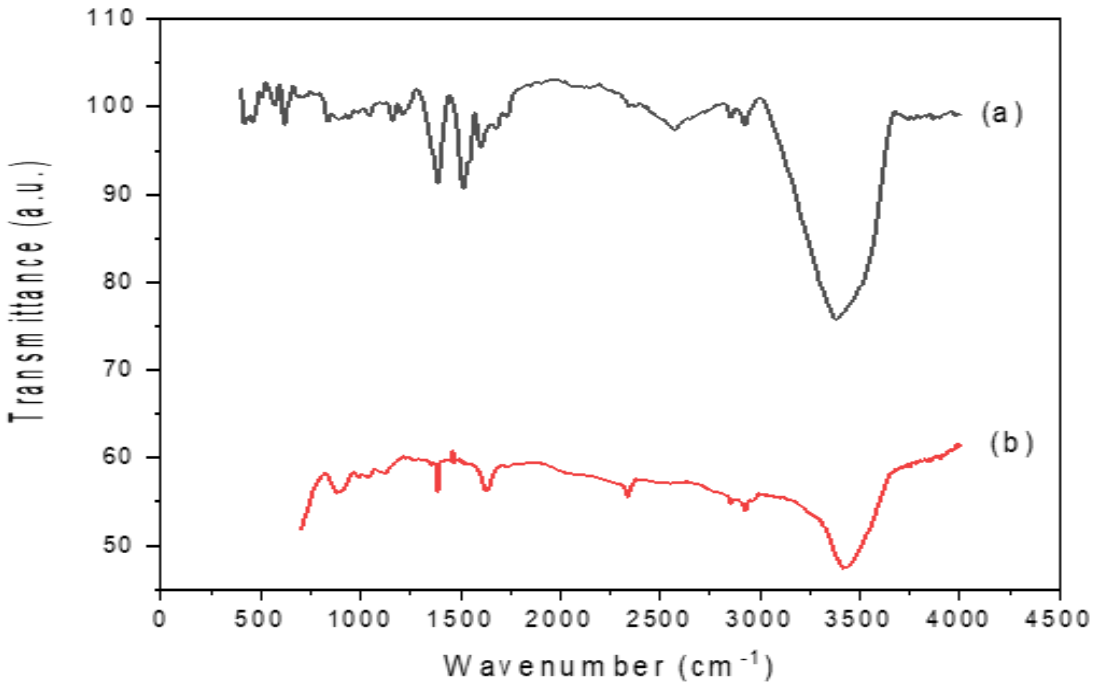

3.1.2. XRD

XRD 20-70° corresponds to highly crystalline composite materials peaks. The diffraction peaks showed no significant variation, confirming that no Ag-ZnO solid solution was generated (figure 9).

Figure 9

XRD analysis results for (a) Ag/ZnO and (b) MOF-Ag/ZnO

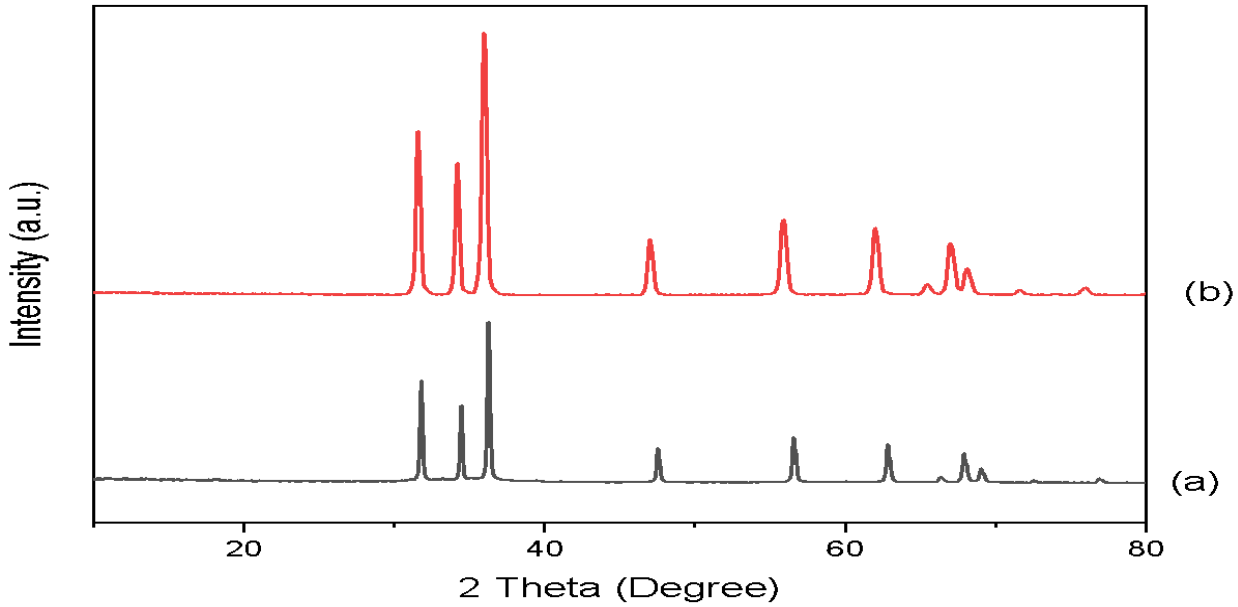

3.1.3. SEM

SEM Image-Based Analysis: The SEM images showed the produced ZnO particles have a spherical structure with approximately 200 nm of diameter. Ag nanoparticles were detected on the surface of the ZnO microspheres, and the MOF layer had little effect on the morphology (figure 10).

Figure 10

SEM analysis results for (a) Ag/ZnO and (b) MOF-Ag/ZnO

(a)

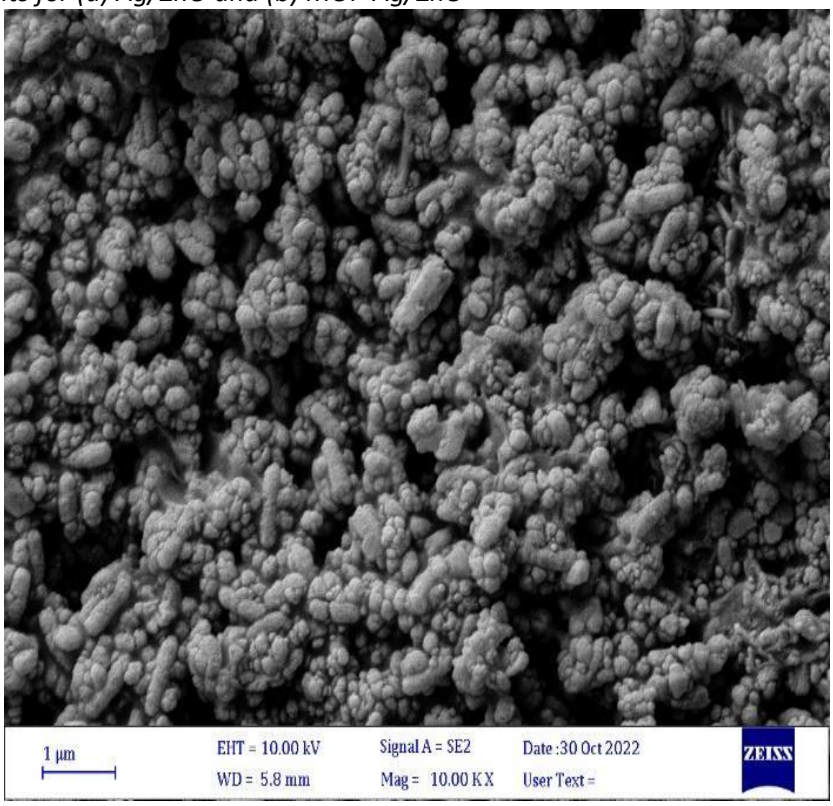

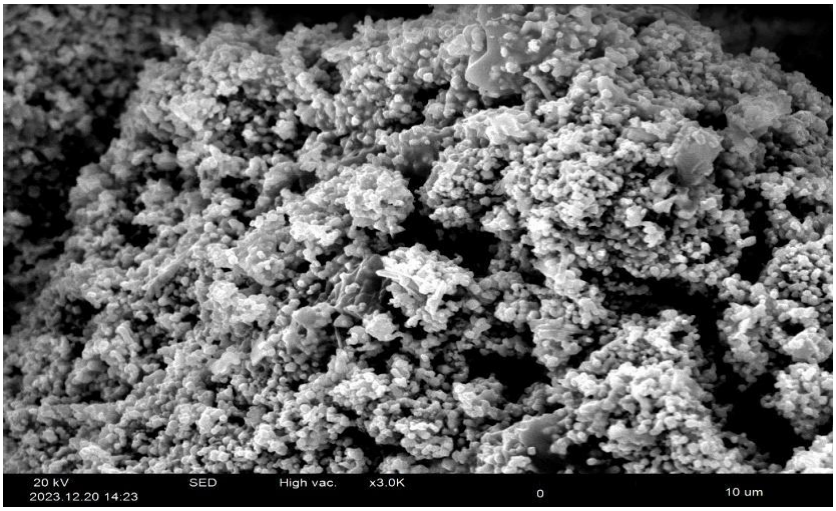

(b)

3.1.4. DRS

DRS Analysis It could be seen from DRS spectra that Ag-ZnO absorbed light almost only in the UV area with an absorption edge of 400 nm. The MOF-Ag/ZnO nanocomposite had extra absorption in the visible range with edges at 600 and 720 nm (figure 11).

Figure 11

DRS analysis results for (a) Ag/ZnO and (b) MOF-Ag/Zn

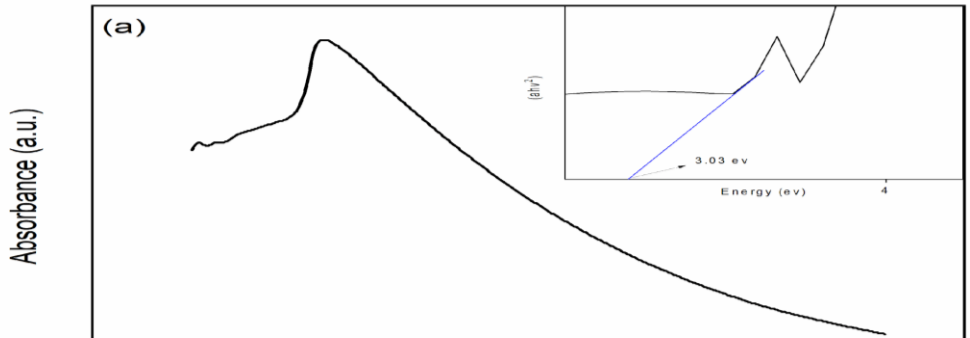

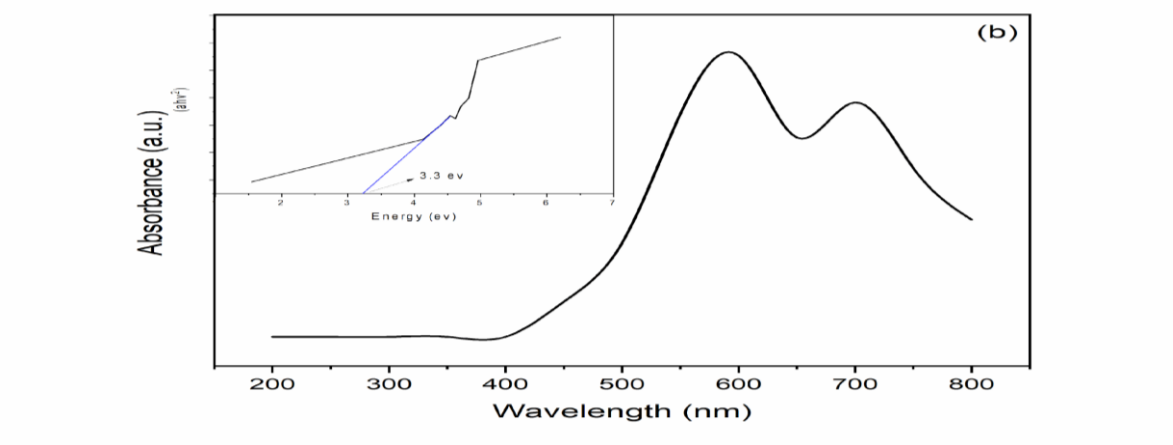

3.2. Photocatalytic tests for dye removal

3.2.1. pH effect

The pH of the solution has a significant effect on the photocatalytic experiment. The anionic dye methyl orange was degraded quickly under acidic conditions where strong adsorption occurred because of the positively charged surface of the catalyst. When a photocatalyst adsorbs at higher density it has many surface hydroxyl groups, and the ionization is greatly affected by pH in the solution. Thus, the only existing active species will be hydroxyl radicals that formed from the reaction of the positive hole (h+) with water and hydroxy groups on an absorbent surface. From there, during the photocatalytic oxidation of dye, adsorption of dye takes place onto hydroxyl groups (OH−) on the surface of the catalyst due to hydrogen bonding. When exposed to UV light, the color diminishes very quickly. Methyl orange is an anionic dye and therefore at low pH, adsorption on the positively charged surfaces can be assumed so the reaction is fast in acidic pH (Ao et al., 2008). Both the normal and alkaline pH were less effective in degrading color than acidic pH (figure 12).

Figure 12

Effect of solution pH on the color reduction process

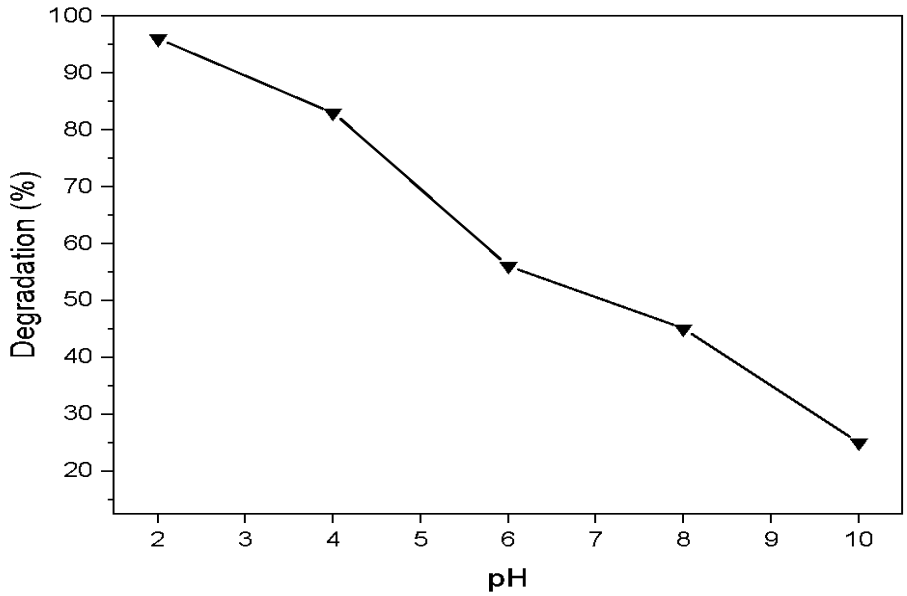

3.2.2. Absorbent dose effect

The removal rate of methyl orange initially increased up to 0.03 g and then decreased. At a small dose of photocatalyst, the photocatalytic reaction is mainly controlled by the active sites that are accessible to absorb light and the reactant, and this may be due to the increase in the number of photons absorbed by the nanocomposite and the number of reactive molecules adsorbed on the photocatalyst with increasing concentration. But after a specific concentration, no other reactive molecules are ready for use for absorption, and hence additional catalysts are not involved in the catalytic activity, with a gradual increase in the photocatalyst dose, the turbidity of the solution increases, which in turn increases the scattering of UV light.

In addition, the increase of UV-light scattering by the suspended photocatalyst significantly reduces the UV transmission and as a result, the photocatalytic color removal is weakened. Therefore, the color removal rate by the catalyst decreases with the increase of the catalyst dose (figure 13).

Figure 13

Effect of photocatalyst dose on the color degradation process

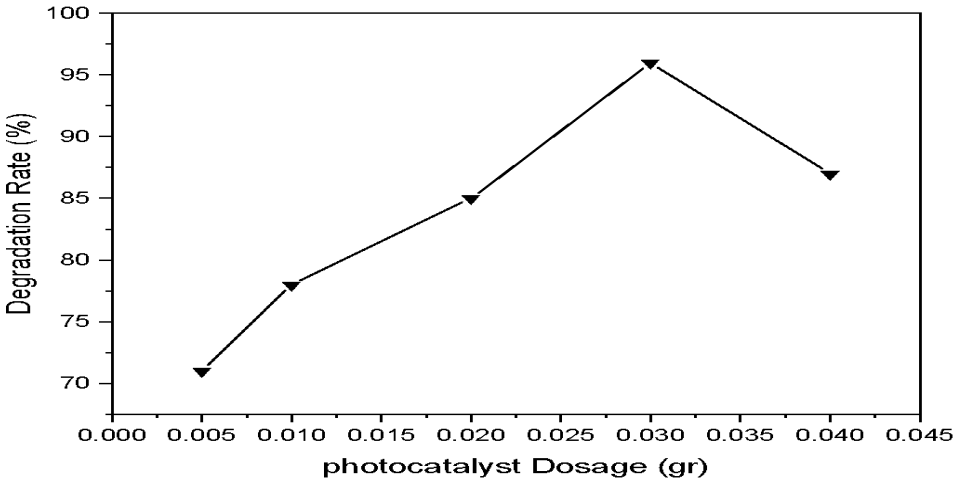

3.2.3. Effect of the initial concentration of the pollution

The initial concentration of the dye greatly affected the degradation rate, recording the maximum removal rate (96% at 30 ppm). Removal efficiencies decreased with the increase in initial concentrations (figure 14).

Figure 14

The effect of the preliminary concentration dye on the coloration discount process

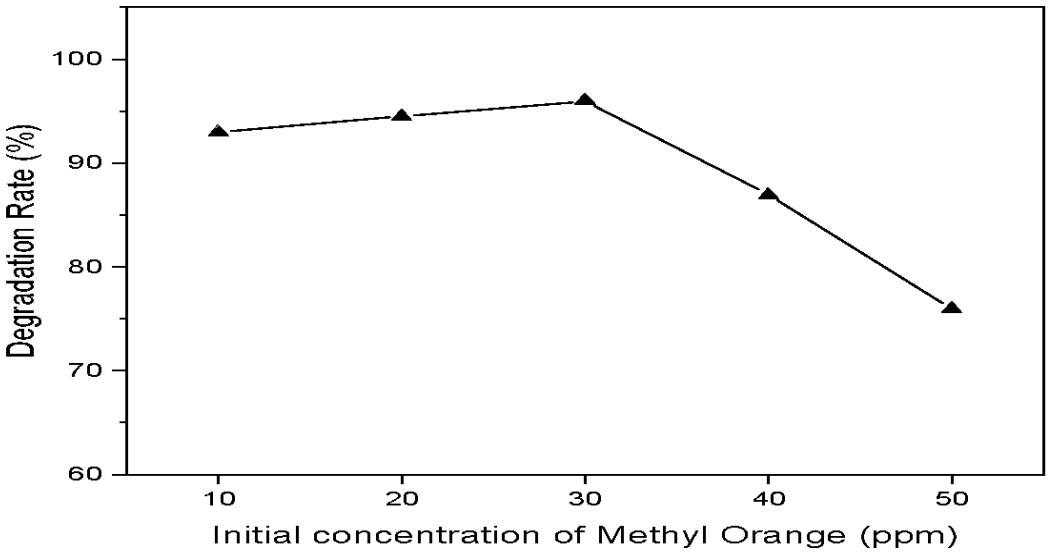

3.2.4. Photocatalyst regeneration

The photocatalyst exhibited excellent removal efficiency, with only a marginal loss of performance recorded after the second cycle. The percentage of dye removal starts at 96% for cycle 1, however, in cycle 2 there is almost a slight decrease in performance of about 5%. To demonstrate a material's ability to be recycled, it is expected that relatively constant activity is maintained for at least the 3 cycles that were present in these tests (figure 15).

Figure 15

Photocatalyst regeneration

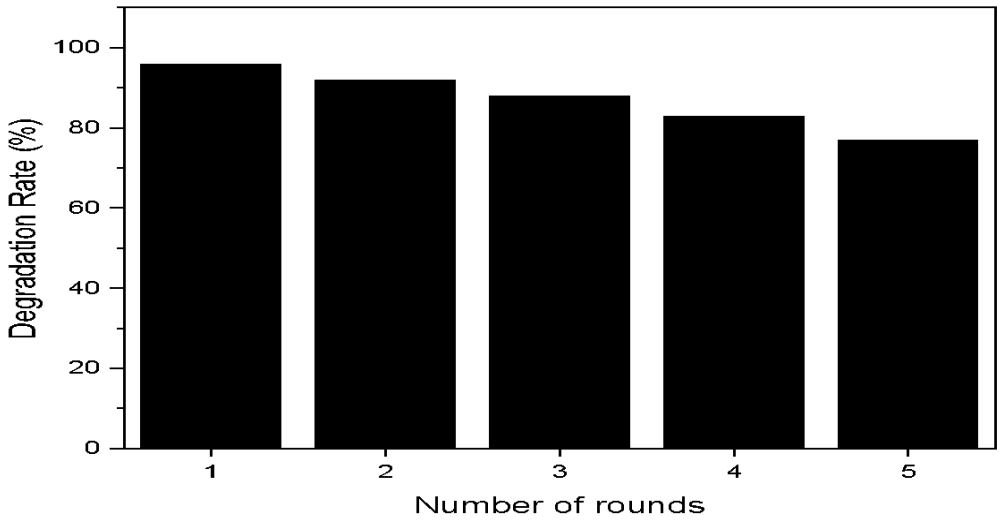

4. DISCUSSION

The characterization and photocatalytic performance of the synthesized Ag-ZnO and MOF-Ag/ZnO nanocomposites reveal significant insights into their structural, optical, and functional properties.

The FTIR spectra confirmed the presence of characteristic functional groups, such as the O-H stretching band at 3444 cm^{-1} and the Zn-O bond at 429 cm^{-1}. Additional peaks at 1384 cm^{-1} and 1576 cm^{-1} validated the presence of carboxylate groups from the MOF structure. These observations indicate the successful synthesis and integration of the MOF layer with Ag-ZnO.

The XRD results demonstrated high crystallinity for the synthesized nanocomposites. The diffraction patterns showed no substantial variations between Ag-ZnO and MOF-Ag/ZnO, confirming that the addition of MOF did not alter the crystal structure of Ag-ZnO or lead to the formation of a solid solution.

The SEM images showed spherical ZnO particles approximately 200 nm in diameter, with Ag nanoparticles distributed on the surface. The MOF layer's minimal impact on morphology suggests that it contributes primarily to the enhancement of photocatalytic activity without significantly altering the structural attributes.

The DRS spectra revealed that Ag-ZnO absorbed primarily in the UV region, while MOF-Ag/ZnO exhibited additional absorption in the visible spectrum, particularly at 600 and 720 nm. This extended absorption range highlights the MOF layer's role in improving the light-harvesting capabilities of the nanocomposite, enhancing photocatalytic performance under broader light conditions.

The pH of the solution significantly influenced the photocatalytic degradation of methyl orange, with acidic conditions (pH 2) leading to a degradation efficiency of 96%. This was attributed to the strong adsorption of the anionic dye on the positively charged catalyst surface. Additionally, the optimal photocatalyst dosage of 0.03 g demonstrated efficient degradation, beyond which turbidity and UV scattering reduced performance. The initial dye concentration also affected removal efficiency, with a maximum of 96% degradation at 30 ppm.

The nanocomposites exhibited excellent reusability, with a slight decline in efficiency (approximately 5%) after the second cycle, demonstrating promising stability and potential for practical applications.

5. CONCLUSION

The synthesized Ag-ZnO and MOF-Ag/ZnO nanocomposites effectively enhanced the photocatalytic degradation of methyl orange under UV and visible light. FTIR, XRD, SEM, and DRS analyses confirmed their structural integrity and superior light-harvesting capabilities. Optimal conditions, including acidic pH, appropriate catalyst dosage, and suitable initial dye concentration, achieved a high degradation efficiency of 96%.

Furthermore, the nanocomposites demonstrated excellent reusability, maintaining performance over multiple cycles. These findings underscore the potential of MOF-Ag/ZnO as a sustainable and efficient solution for water purification and industrial dye removal. Future research could explore scaling up the process and testing with real industrial effluents to further validate practical applicability.

Conflict of interest: No potential conflict of interest was reported by the authors.

Ethical Approval: The study adheres to the ethical guidelines for conducting research.

Funding: This research did not receive any specific grant from funding agencies in the public, commercial, or not-for-profit sectors.

Hameed, H.M., Hasan, I.A. & Awad, A.T. (2024). Synthesis of Ag-ZnO/MOF nanocomposite for degradation of dye from aqueous solution under UV light. *World Journal of Environmental Research*, *14*(2), 131-144. https://doi.org/10.18844/wjer.v14i2.9589

REFERENCES

Ao, Y., Xu, J., Fu, D., Shen, X., & Yuan, C. (2008). A novel magnetically separable composite photocatalyst: titania-coated magnetic activated carbon. *Separation and Purification Technology*, *61*(3), 436-441. https://www.sciencedirect.com/science/article/pii/S1383586607005667

Gao, W., Zhong, M., & Su, B. (2024). Hydrogel-Based Photocatalysts: Applications in Environmental Remediation and Energy Conversion. *Journal of Polymers and the Environment*, 1-18. https://link.springer.com/article/10.1007/s10924-024-03379-2

Hashem, A. A., El-Wahab, A., Selim, M. M. A., & Badawy, A. A. (2024). Nanozinc ferrites@ silica as efficient adsorbent for dye removal from wastewater: synthesis and adsorption studies. *International Journal of Environmental Science and Technology*, 1-17. https://link.springer.com/article/10.1007/s13762-024-05564-1

Kiteto, M., Vidija, B., Mecha, C. A., Mrosso, R., & Chollom, M. N. (2024). Advances in metal-organic frameworks as adsorbents, photocatalysts, and membranes: a new frontier in water purification. *Discover Water*, *4*(1), 54. https://link.springer.com/article/10.1007/s43832-024-00119-4

Latif, S., Alanazi, K. D., Alshammari, B. H., Al-Ahmed, A., & Alanazi, A. M. (2024). Utilization of river tamarind stem driven biochar for efficient removal of phenol dye from polluted water: insights from adsorption studies. *Biomass Conversion and Biorefinery*, 1-15. https://link.springer.com/article/10.1007/s13399-024-05741-9

Sharma, V. P., & Sharma, P. (2021). Environmental contaminants: treatment, threats, toxicity, and tools for sustainability. In *Wastewater treatment* (pp. 93-102). Elsevier. https://www.sciencedirect.com/science/article/pii/B9780128218815000052

Sheng, J., & Webber, M. (2021). Incentive coordination for transboundary water pollution control: The case of the middle route of China's South-North Water Transfer Project. *Journal of Hydrology*, *598*, 125705. https://www.sciencedirect.com/science/article/pii/S0022169420311665

Singh, A., Tomar, R., & Singh, N. B. (2024). Efficient removal of crystal violet dye from water using zinc ferrite-polyaniline nanocomposites. *Environmental Monitoring and Assessment*, *196*(6), 1-18. https://link.springer.com/article/10.1007/s10661-024-12686-z

Srivastav, A. L., Rani, L., Sharda, P., Patel, A., Patel, N., & Chaudhary, V. K. (2024). Sustainable biochar adsorbents for dye removal from water: present state of the art and future directions. *Adsorption*, *30*(7), 1791-1804. https://link.springer.com/article/10.1007/s10450-024-00522-2

Suriadikusumah, A., Mulyani, O., Sudirja, R., Sofyan, E. T., Maulana, M. H. R., & Mulyono, A. (2021). Analysis of the water quality at Cipeusing River, Indonesia using the pollution index method. *Acta Ecologica Sinica*, *41*(3), 177-182. https://www.sciencedirect.com/science/article/pii/S187220322030192X